Design of nanoengineered hybrid PVA/PNIPAm/$CaCl_2$/SiO_2-Polystyrene (PSt) colloidal crystal hydrogel coatings that sweat/rehydrate H_2O from the atmosphere to give sustainable cooling and self-indicate their state

Jean-Charles Eloi, Myles P. Worsley and Paul A. Sermon*
Nanomaterials Laboratory, Wolfson Centre for Materials Processing, Brunel University, Uxbridge, Middlesex UB8 3PH, UK
William Healy and Christine Dimech
Dstl Fort Halstead, Sevenoaks, Kent TN14 7BP, UK

Abstract

The potential for nanoengineering hybrid PVA hydrogel and hydrogel microsphere optical coatings is demonstrated with fine-tuning by the addition of (i) PNIPAm domains, (ii) water-hunting humectant $CaCl_2$, and (ii) polystyrene or SiO_2 colloidal crystals. The design and application onto substrates of the hydrogel scaffold is described. The addition of a temperature-triggered component as well as humectant and NIR reflectors are reported. The hybrid hydrogels appeared effective in sustainable adsorption cooling technology (ACT) over sustained periods. It is shown that the thermoresponsive (PNIPAm) domains act as an extra reserve, sweating water above 305K, prolonging the controlled release of water. It is also reported that the addition of humectant is crucial for the natural re-hydration of the hydrogels. For the moment PNIPAm microspheres have only short-lived ACT properties. Finally, coating with microspheres (MSs) in hydrogels produces a visible-NIR reflector effect that may allow optical feedback on ACT.

Keywords: hydrogels, PVA, adsorption cooling, microsphere, IR, green technology, optical coating

1. Introduction

Space heating/cooling accounts for 30% of energy consumption and one way to make this greener is through adsorption cooling technology (ACT) which has a lineage that stretches back to Michael Faraday [1]. Thermally driven adsorption chillers enable low grade heat to drive refrigeration cycles. These may use data centre heat, process heat [2] or solar/photovoltaic [3] sources and their operation is often intermittent, but they can produce significant energy savings. Many ACTs are based on exothermic adsorption-endothermic desorption with water on silica [4], templated SiO_2 [5], metal aluminophosphates [6], zeolites [7], MOFs or carbon [8]. Sometimes the adsorbents have hygroscopic salts (e.g. $CaCl_2$ or LiBr) [9] added. The extent and rate of water adsorption/desorption can be followed in real-time cycling with intervals of 300s [4] at a selected % relative humidity (RH) and temperature (T). A commercial SiO_2/water 15kW cooling unit lowers the temperature of inlet water from 328K to 305K in 10 stages [10]. The specific cooling power (SCP) is a measure of efficiency. The authors were surprised that hydrogels (with their high water content and ability to host nanoparticles (NPs)) had not been evaluated in this context; they were interested here to know if

(i) thermoresponsive [11,12] polymers (poly(N-isopropylacrylamide) or PNIPAm) with low critical solution temperatures (LCST) (305K) [13], below which they are hydrophilic, but above which they are hydrophobic, could cause the hydrogels to contract/expel water [14] (i.e. mimicking animal sweating) [15] thereby increasing ACT performance or

(ii) photonic crystals, that may be present on the skin of chameleons [16] renowned for their camouflage

could modify hydrogel ACT properties of IR feedback on performance (IR reflectors [17]).

Nanophotonic Materials XIII, edited by Stefano Cabrini, Gilles Lérondel, Adam M. Schwartzberg, Taleb Mokari, Proc. of SPIE Vol. 9919, 99190V
 · doi: 10.1117/12.2237561

Our objective here was to produce PVA-based hydrogel coatings. PVA was chosen because it is water soluble/deliverable, thermally stable to 493-513K [18], non-toxic even on human ingestion [19] and non-skin-sensitizing.

Specifically, here we wished to explore the ACT properties of hydrogel coatings produced from aqueous solutions/suspensions with varying levels of glutaraldehyde (GLA)-chemical and thermal-physical crosslinking that contained

- water-hunting humectant $CaCl_2$ [8,9],
- PNIPAm [20] sweating domains, and
- biomimetic photonic colloidal crystal structures [21,22] .

In a feedback sense we wanted to probe these in the NIR (0.75-1.4μm) and LWIR (3-15μm) during their sustainable water adsorption/desorption cycling over more than 24h as %RH and T varied (where exothermic sorption is inversely proportional to temperature) [23]. It was hoped that these modified hydrogels could be applied to polymer and metal surfaces by spraying or painting over mm^2 or m^2 areas. Preliminary results are now reported for the first time.

2. Experimental

2.1 Materials

All chemicals were purchased from Sigma Aldrich. Deionised water (18.2Mohm.cm) was used exclusively throughout. PVA hydrogels (physically- and chemically-crosslinked) or colloid-modified hydrogel samples had varying levels of cross-linking. Some hydrogels were prepared with NIPAm dispersed in the PVA aqueous solution, to which was added a crosslinker (*N*,*N*'-methylene-bis-acrylamide) or not, a radical initiator (ammonium peroxodisulfate) and an accelerator (*N*,*N*,*N*',*N*'-tetramethylethylene diamine) [15]. Some hydrogels contained polystyrene (PSt) or SiO_2 colloidal particles or microspheres (MS). SiO_2 and PSt colloidal particles were prepared as described [24,25] and used as photonic crystal models as previously [25]. These were characterized by optical microscopy and SEM (Zeiss Supra 35VP)-EDX. DSC measurements were performed on a Q2000 from TA instruments: a few mg of a dried hydrogel coating was placed into the DSC cell with a $100mm^3$ H_2O reservoir under a $5cm^3$/min N_2 steady flow. The heat flow was recorded over time. Hydrogel coating IR signatures were recorded using cameras listed in Table 1. Dispersed 1-4μm diameter PVA hydrogel microspheres were also produced [26] as follows: (i) $40cm^3$ 8%$PVA_{(aq)}$ solution was heated to 343K and then 2g Span 80 was added, followed by $80cm^3$ octane to form a water-in-oil emulsion, (ii) PVA microspheres were chemically cross-linked by first adding $0.2cm^3$ 100mM $HCl_{(aq)}$ followed by $8cm^3$ 25%$_{(aq)}$ GLA and (iii) the whole was left stirring at 343K for 2h. PNIPAm hydrogel microspheres have also been prepared by co-polymerizing N-isopropylacrylamide (NIPAm) and N,N,N-methylene-*bis*-acrylamide (MBAM) in an aqueous reflux [27]. In general, NIPAm (e.g. 2.5g) was dissolved in 100-150cm^3 water at 343K along with 10% MBAM (by mass to NIPAm). The polymerisation was initiated by the addition of 50mg of potassium persulfate ($K_2S_2O_8$) and left under reflux for 2-15h in a N_2 atmosphere. The PVA hydrogel microspheres self-assembled into close-packed structures. Typical hydrogel dimensions are that of PSt substrate (88mm disc of 3.0-3.5mm thickness) and borosilicate glass microscope slides (75mm x 25mm, τ=1mm), after cleaning with ethanol.

2.2 Description of experimental set-up (shown schematically in Figure 1)

The samples were held at either 318-323K or 277K to simulate daytime release of H_2O and night-time recovery of water and cycled between these at intervals. The samples were placed inside a dark matt box to avoid stray IR (NIR/SWIR/LWIR noise); water content changes were measured gravimetrically. Table 1 summarizes systems used for IR analysis. The samples were imaged in real time with this instrumentation. The uncoated PSt substrate surface showed no ACT effect. The hydrogel coatings on this substrate that were tested here are shown in Table 2.

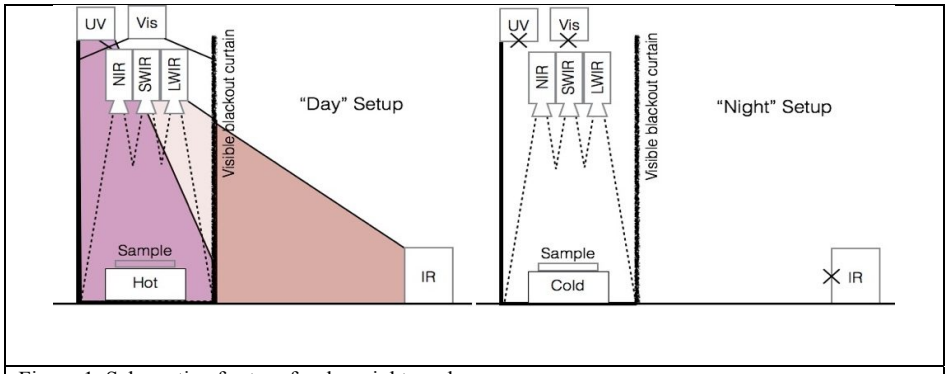

Figure 1. Schematic of set up for day-night modes

Table 1. Specifications for IR imagers

Manufacturer	Model	Infrared Spectrum	Acronym
Olympus	Modified	Visible to ~650-700 nm	Vis-NIR
Pyser-SGI limited	PNP-HG	Near infrared 350-900 nm	NIR
XenICs	XS-514	Shortwave infrared 900-1700 nm	SWIR
Cedip	Emerald E660	Midwave infrared 3600-5000 nm	MWIR
FLIR	Thermacam PM695	Longwave infrared 7500-13000 nm	LWIR

3. Results

3.1 Silica (SiO_2), polystyrene (PSt) colloidal particle/microsphere (MS) synthesis, characterization and assembly into colloidal crystals

SiO_2 microspheres of 300nm diameters formed colloidal crystals (see Figure 2A,B) that gave long-UV to visible response at different wavelengths, depending on the angle of viewing.

Larger polystyrene (PSt) microspheres (average 900nm in diameter) were characterized by optical and electron microscopy after they had been fabricated into colloidal crystals by centrifuging, dip-coating and assembly at 2D air-liquid interfaces (see Figure 3A,B). In the 3D colloidal crystals the latex particles order locally in an expected hexagonal compact way, but with some domains exhibiting cubic packing and short range order. Factors that influence the degree of ordering included dispersant, microsphere concentration and substrate properties. Although not completely close-packed and containing defects, these PSt colloidal crystals showed significant reflectance 550-750nm (see Figure 3C) in the visible-NIR. Smaller 400nm PSt microspheres (but not those of 900nm or SiO_2) showed significant absorption at 610nm (see Figure 4A). There was an angular component of their response in that transmitted light, incoming at 90° and 45° angles, produced a photonic diffraction response that was centered around the NIR region (see Figure 4B).

Figure 5 shows that close-packed μm-sized hierarchical structures and corrugations seen with MSs of varying refractive index could be included within our PVA hydrogel coatings, introducing interesting optical or IR properties.

3.2 PVA and PNIPAm hydrogel microsphere synthesis, characterization and coating

PVA microspheres were also prepared from a Span 80-stabilised water-in-octane microemulsion and PNIPAm ones from polymerization under reflux in an N_2 atmosphere. These were successfully applied to surfaces, modifying their LWIR imaging. It is assumed that on the substrate surface they form hemi-microspheres (HMSs), with a concentration that can be controlled. Self-assembled PVA hydrogel microspheres (1- 4μm diameter) were characterized by optical and

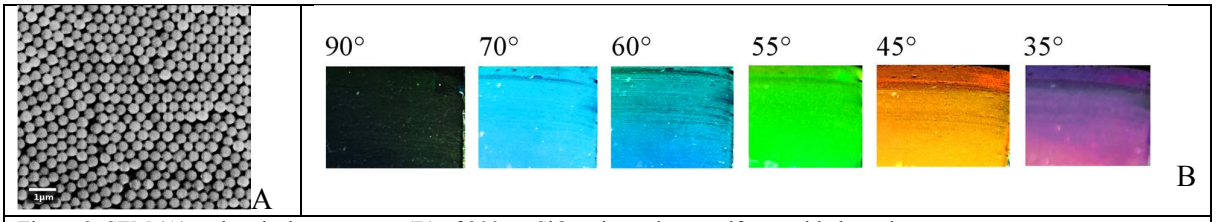

Figure 2. SEM (A) and optical appearance (B) of 300nm SiO_2 microspheres self-assembled on glass.

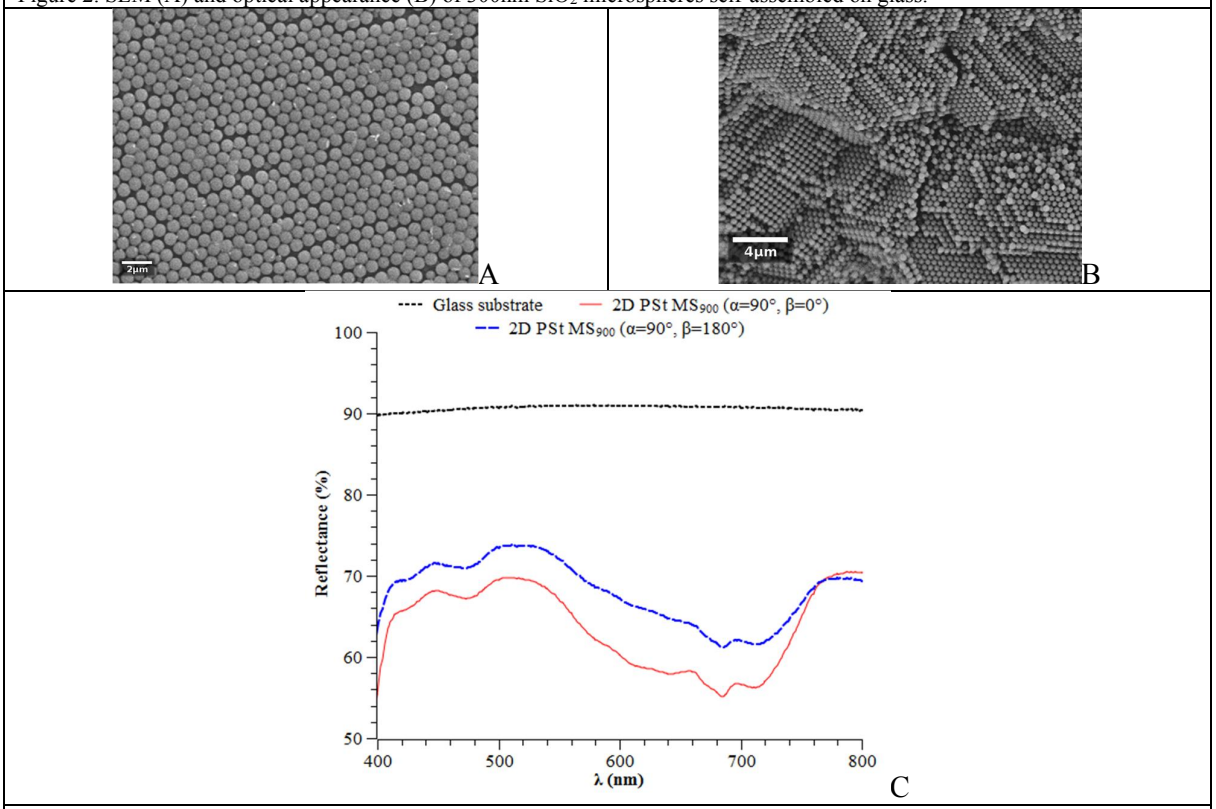

Figure 3. SEM (A,B) and reflectance (C) of polystyrene (PSt) microspheres (MSs)

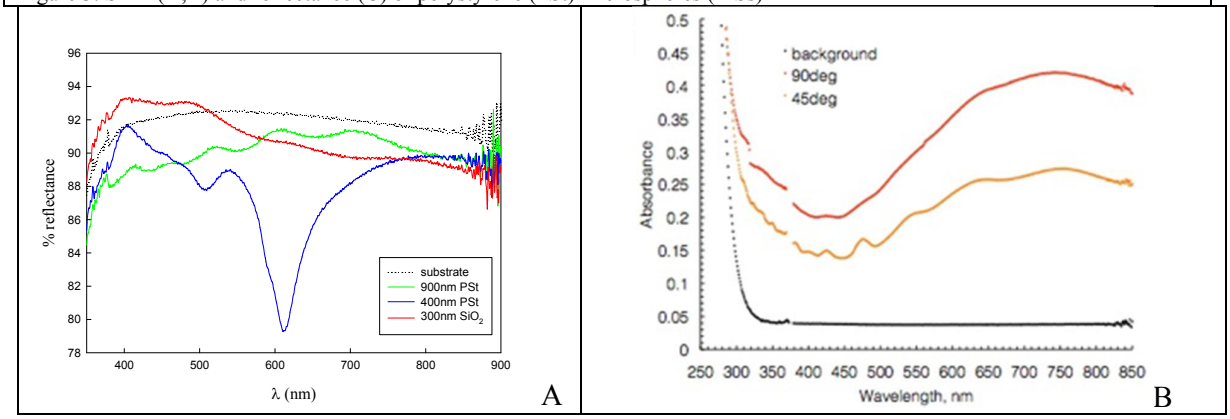

Figure 4. UV-vis-NIR reflectance (A) and absorbance (B) responses of 3D arranged PSt and SiO_2 microspheres produced by spin-coating at 2500rpm at different angles of incidence.

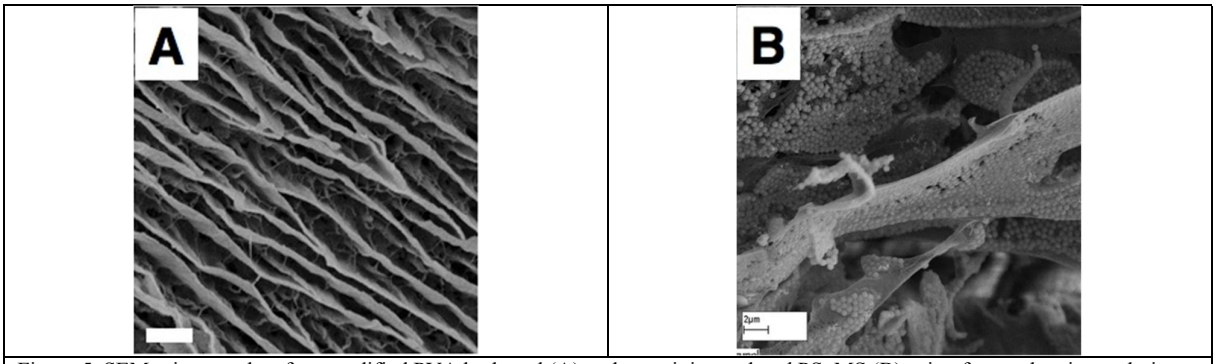

Figure 5. SEM micrographs of un-modified PVA hydrogel (A) and containing ordered PSt MS (B) using freeze-thawing techniques to orient the particles locally.

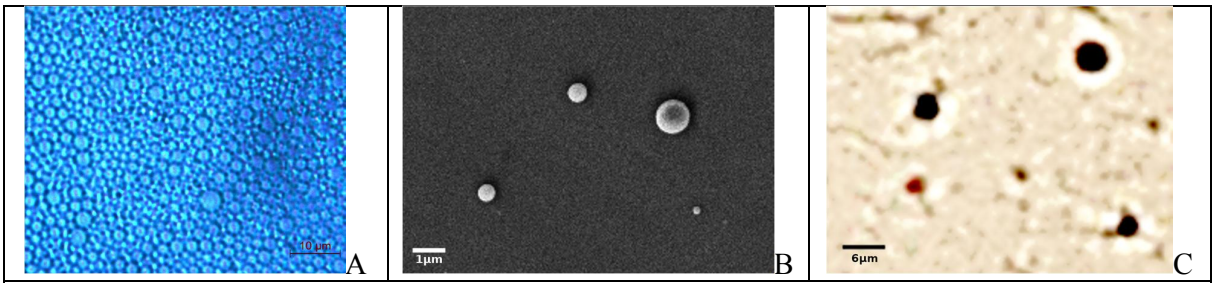

Figure 6. Optical (A) and SEM (B) micrographs of PVA hydrogel microspheres. Optical micrograph of PNIPAm microspheres (C)

Table 2. Samples tested

Sample	Description	Measurement Description (D=day; N=night)	Sensors
1	PVA hydrogel	Over 12 days with natural hot and cold (D + N) cycles and 2 re-hydration at day 4 and day 8	LWIR
2	PVA/PNIPAm hydrogel	Over 3 days with natural hot and cold (D +N) cycles. Re-hydration performed post cycles. 3 cycles of hot and cold (artificial D + N)	NIR, SWIR, LWIR
3	PVA/PNIPAm/$CaCl_2$ humectant	cycles, isotherms, multi angle DSC, and SEM	LWIR, SWIR (and DSC, SEM)
4	Sprayed PNIPAm microspheres	3 cycles of hot and cold (artificial D + N)	NIR, SWIR, LWIR

electron microscopy (see Figure 6A,B). The authors intend to ascertain the extent of any crosslinking by ^{1}H and ^{13}C-NMR. PNIPAm microspheres were investigated for their ACT properties.

3.3 Water loss and recovery from nanoengineered hybrid hydrogel coatings and ACT

Experiments were now aimed to study the daytime water loss and night time H_2O recovery of the above nanoengineered hybrid hydrogel coatings in real-time in a simulation of shortened cycles of night and day, while monitoring *in situ* IR outputs (NIR, SWIR and LWIR), in order to assess ACT potential.

Real-time LWIR analysis of PVA hydrogel coatings alone (sample 1) revealed that they dried over 3 days (see Figure 7). Nevertheless they acted as a scaffold reservoir that had an ability to slowly release water over time with ACT benefits. The temperature difference (ΔT) in night and day is in the order of 4K (green curve), but at point C this capacity is largely exhausted. However, at points D and E the hydrogel coating was effectively and rapidly rehydrated. It appears then that PVA hydrogel coatings could well represent a sustainable ACT opportunity on a variety of substrates. The next step was now to determine whether additional water reserve capacity and easier rehydration could be improved through hydrogel modification.

In sample 2, the addition of 7.5% of a thermo-responsive polymer (PNIPAm) to the crosslinked PVA hydrogel was explored. This had the effect of allowing a better, more thorough re-hydration (83.7%; see Figure 8) and sustaining the period of effective ACT use of the hydrogel (i.e. it now operated over >3 days of natural day and night cycles, with no rehydration step). The reader needs to note that the local temperatures (from the MET office; plotted in orange) decreased gradually from 3000 minutes, that is related to the decrease in outdoor temperature (i.e. the coating was not air-conditioned). However, the ΔT between ambient and the hydrogel is lower than with PVA alone, despite more water being retained and released over longer periods. It was possible to predict the water loss (red curve) from previous water loss trends, by integration of the temperature-dependent rate $r(T)$ over time: $\int r(T).\mathrm{d}t$. Hence, PNIPAM addition is beneficial in an ACT sense.

In sample 3, the addition of a humectant (i.e. $CaCl_2$) was explored to determine whether it enhanced the hydrogel intake and release of water. When subjected %RH>32%, this humectant absorbs water, regardless of the external temperature. This process was studied with hydrogel using DSC in an isothermal manner (at 293K) where the thermo-responsive polymer component is hydrophilic. Figure 9 shows heat flow plots of the background (furnace cell) and of the hydrogel. No clear endothermic or exothermic 1st or 2nd order transition peaks are observed during the hydration phase. However, the heat flow ($\mathrm{d}H/\mathrm{d}t$) was not constant and can be described as $\mathrm{d}H/\mathrm{d}t = Cp \times \mathrm{d}T/\mathrm{d}t + f(T,t)$, were Cp is the sample's heat capacity and the kinetic heat flow term is $f(T,t)$. As we are performing isotherms, $\mathrm{d}T/\mathrm{d}t = 0$. Hence the heat flow is only the kinetic heat flow term $f(T,t)$ and can be written $\mathrm{d}H/\mathrm{d}t = \mathrm{A}(T) \times t + \mathrm{B}(T)$, where A and B only depend on T, which is fixed here. Because T is fixed, only the heat capacity of the sample is varying in a linear manner. This is due to the change in the sample's Cp from dry to wet to saturated. The saturation is indicated by the sudden change of slope at t =120 min, after which the heat flow is constant. The global mass change between dry and saturated indicates that the hydrogel coating doubles its weight by absorbing its own weight in water, creating a gram for gram water reserve.

This sample (3; consisting of scaffold and water reserve PVA hydrogel, temperature-triggered extra water reserve PNIPAm, and humectant $CaCl_2$ for water recovery) has been subjected to various substrates temperatures and the observed coating temperature recorded and plotted in Figure 10.

At low temperatures (Figure 10A), this modified hydrogel coating follows the substrate's temperature as there is no significant difference between coating and substrate. This is important; this is when the coating is recharging itself with moisture present naturally in air (*e.g.* early morning dew for outdoor applications). It is only when it is subjected to higher temperatures (isotherms Figure 10B or cycles Figure 10C) that the thermoresponsive component releases water controllably, with the effect of lowering the coating temperature. Moreover, the water present in the hydrogel is evaporated faster at higher temperatures.

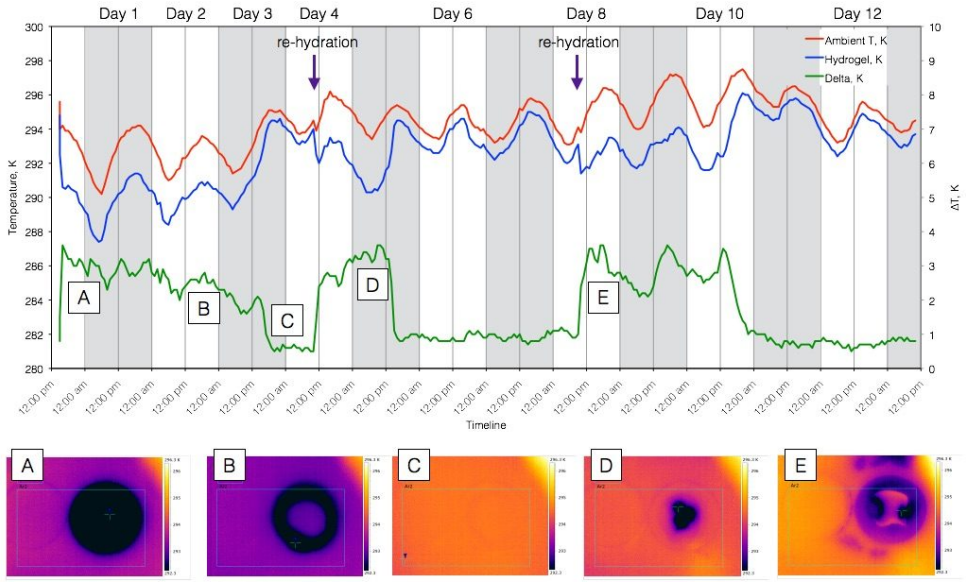

Figure 7. ACT data (top) and LWIR images (bottom) for PVA hydrogel (sample 1) over 12 days as it was subjected to natural day and night temperature cycles with 2 re-hydrations at day 4 and day 8

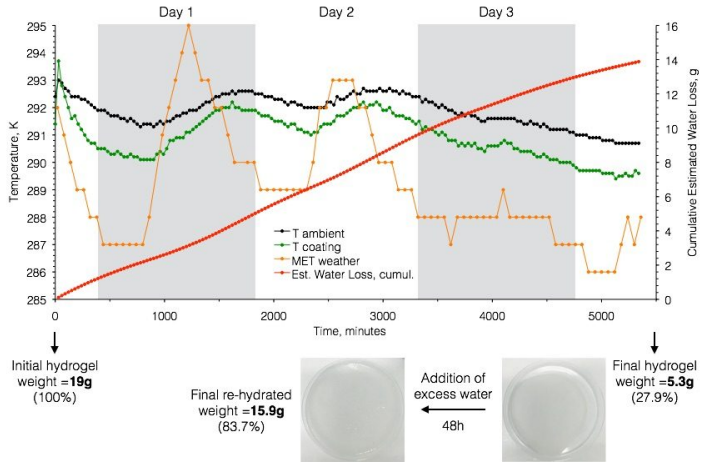

Figure 8. ACT data for PNIPAm-modified PVA hydrogel (sample 2) over more than 3 days with natural hot/cold cycles; re-hydration images and data are after 3.5 days.

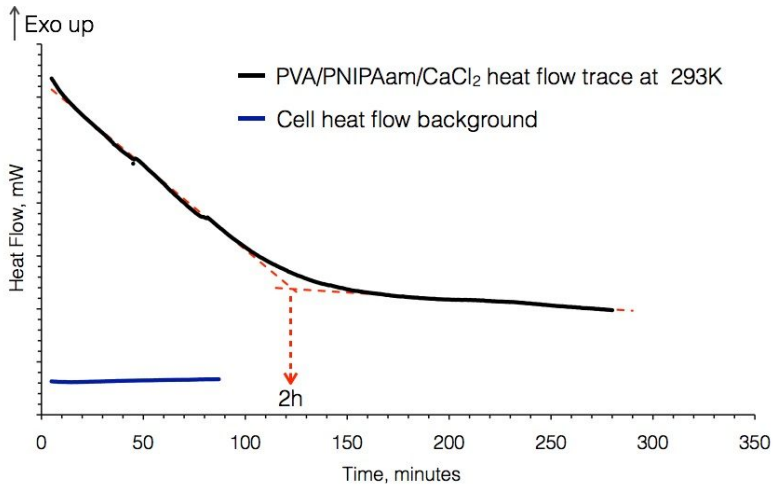

Figure 9. DSC plots of the water intake of sample 3 from dry (t=0min) to saturated (t>300min)

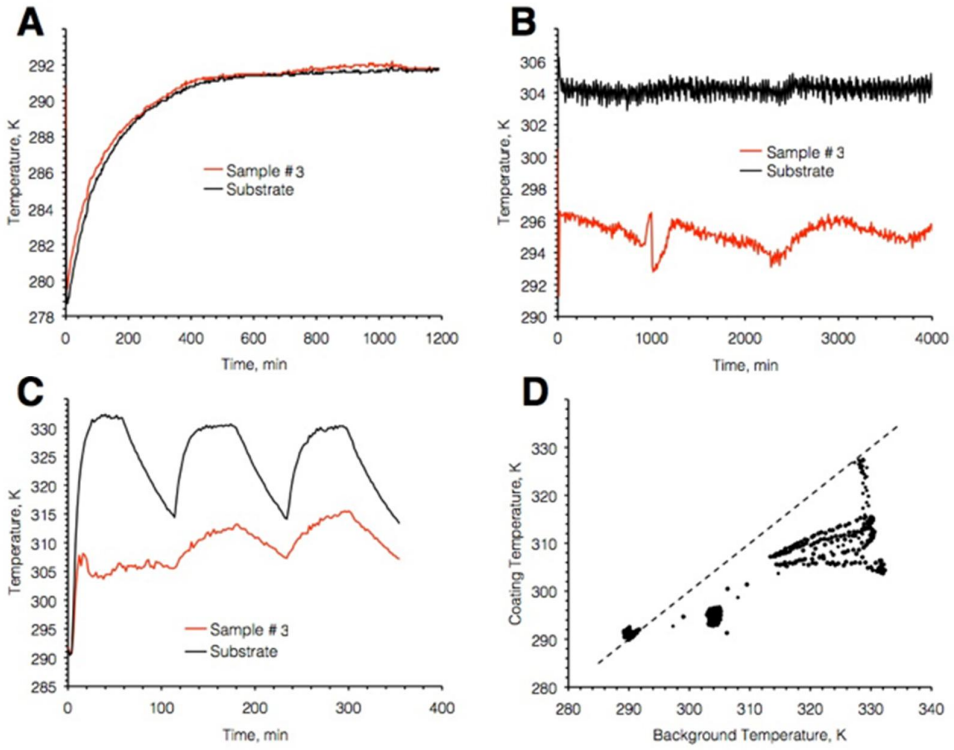

Figure 10. Plots of the response of sample 3 to various substrate temperatures (A to C) and all the data combined in (D)

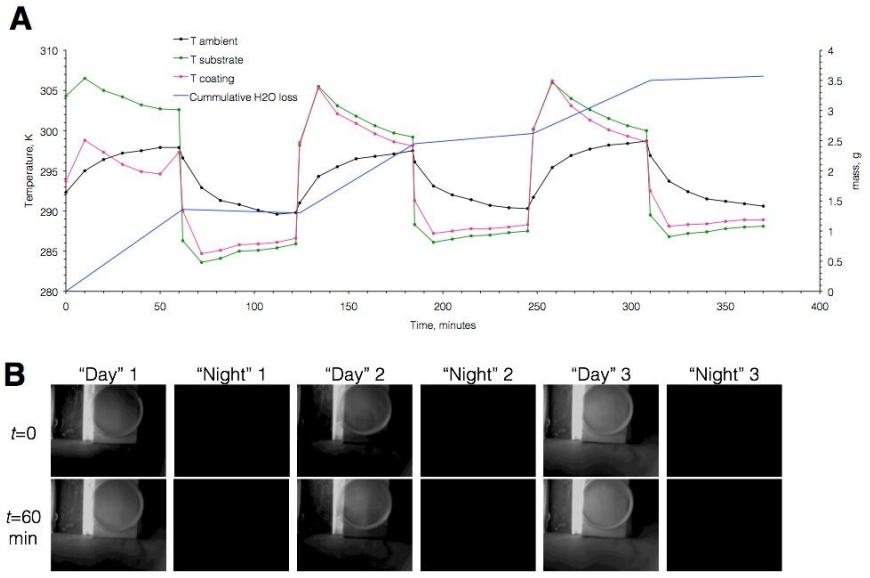

Figure 11. ACT data for a PNIPAm hydrogel microsphere (MS)-based coating (Sample 4) (A) and SWIR images (B)

All data relating the coating temperature to that of the background are plotted together in Figure 10D. It is clear that for almost all temperatures between 290 and 330 K, the coating temperature was well below those of the substrate. This is only possible, independent of the substrate temperature, when the coating has some water in reserve. If not, the coating will reach the substrate's temperature (as observed at background temperature of 330K in Figure 10D, where, over time, the coating reached the dashed line). At this point, as seen in Figure 9, the coating will recharge fully in 2 h.

3.3 Water loss and recovery from nanoengineered PNIPAm hydrogel microspheres in ACT simulated with artificial hot day and cool night cycles

Following their study of cycles of natural day and night, the authors addressed the release and recovery of water under hotter and cooler conditions with real-time visible-LWIR analysis. Here, a thinner coating of hydrogel MSs (sample 4) that had been freshly coated from water (containing purely thermo-responsive PNIPAm microspheres) has been investigated (Figure 11). Here, the wt% hydrogel on the substrate was only 25% of samples 1 and 2. Unfortunately, ACT effects (which were significant) were largely lost in the first cycle.

Interestingly, when combined with the hydrogel scaffold, and subjected to the same hot and cold cycles, the coating (sample 2; Figure 12) behaves as intended: a constant, positive temperature difference between substrate (green curve) and coating (red curve) during hot (305K) cycles, accompanied with a predictable water loss (blue curve), followed by matching temperatures during cooler cycles (285K), with no water loss. The authors would like to point that water intake happens mainly when the coating approaches water depletion.

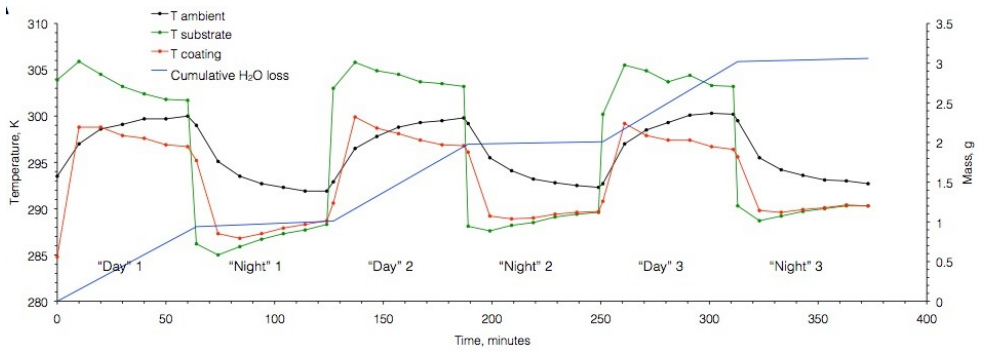

Figure 12. ACT data for a PVA/PNIPAm hydrogel coating (Sample 2)

4. Discussion and conclusions

The ability of an adsorbent to desorb and re-sorb water controllably is a key function in adsorption cooling technology (ACT). A series of daytime and night time phase conditions have been performed on selected hydrogels that consisted of one or several of the following: PVA hydrogel, thermo-responsive polymer and humectant.

All coatings were subjected to temperature and UV, visible and IR light conditions and their responses were measured over a wide range of the IR spectrum (from near to long wavelength).

From the results presented, it is judged that these nanoengineered coatings were green, biocompatible and hydrophilic polymer networks (hydrogels). It has been shown that the amount of water can be designed carefully to match location-dependent conditions (T and %RH). The coating thickness can be controlled on a variety of substrates. These operate even when they appear dry at their surfaces. Indeed, no disastrous irreversible network collapse was seen at extremes of t, T or %RH. Interestingly, when the temperature dropped below 273 K, there was a reinforcement of hydrogel crosslinking (that will be quantified in forthcoming ^{1}H NMR) confining the same amount of H_2O into smaller hydrogel cells [28]. Adding PNIPAm or $CaCl_2$ was beneficial. The added components allowed water to be squeezed out further from the coating at physiological temperature, reversibly; this then was the real purpose of adding the thermo-responsive polymer. The humectant addition allowed water recharge at any temperature, provided a minimum of 32%RH was in the atmosphere, over a 2h period, adsorbing a gram of water per gram of dry coating.

Coatings of close-packed SiO_2 or polystyrene spheres of uniform size have been shown to be self-assembled on a substrate to form 2D rafts or 3D clusters; these are ordered close-packed colloidal crystals. Factors that influence the degree of ordering appear to include dispersant, MS concentration and substrate properties. Using MS materials of varying refractive index, will in future lead to microstructures and corrugations that will give hydrogel coatings IR reflective/photonic properties. Scattering or reflectance in the IR at chosen wavelengths have been seen. These could be introduced into the hydrogels, affecting visible-NIR reflectivity and IR feedback.

PNIPAm microspheres did not show sustainable ACT properties. In the future an alternative route to photonic responses may be shown to be to use stable suspensions of PVA hydrogel microspheres (prepared from Span 80-stabilised water-in-octane microemulsions) that could be applied to *and* self-assemble on surfaces, where they would rapidly dry as fast-assembling 2D photonics crystals that released/took up water visible-NIR-SWIR-LWIR characteristics. At the time of this preliminary report, these do not have as good a period of ACT operation as complete hydrogel coatings.

Hydrogel coatings are used in reverse osmosis desalination [29], stimuli-responsive nano-antennae [30] and medicine [31] and can be generated from sprayed colloidal microspheres [32] to give interesting optical properties, but the sprayable designer IR-active hydrogel coatings described here remain novel. We expect to hear more of hydrogel-based ACT technology that has an in-built optical feedback to define its state of operation.

5. Acknowledgements

The Dstl for support for JCE and MPW under ITT–R1000094462 and DSTLX-1000085816 is gratefully acknowledged.

6. References

[1] Askalany, A.A. 'Hybrid adsorption cooling systems–An overview' Renew.Sust.Energy Rev. 16,5787-5801 (2012)

[2] Chekirou, W., Boukheit, N., and Karaali, A. 'Heat recovery process in an adsorption refrigeration machine' Internat.J.Hydr.Energy 41,7146-7157 (2016)

[3] Garcia-Heller, V., Paredes, S., Ong, C.L., Ruch, P. and Michel, B. 'Exergoeconomic analysis of high concentration photovoltaic thermal co-generation system for space cooling' Renew.Sustain.Energy Rev. 34,8-19 (2014); Xu, S. 'Experiment on a new adsorption bed about adsorption refrigeration driven by solar energy' Energy Proc. 14,1542-1547 (2012); Hassan, H.Z. 'Thermodynamic analysis and theoretical study of a continuous operation solar-powered adsorption refrigeration system' Energy 61,167-178 (2013); Escher, W. 'Thermal management and overall performance of a high concentration PV' AIP Conf.Proc. 1477,239-243 (2012)

[4] Sakoda, A. and Suzuki, M. 'Fundamental study on solar powered adsorption cooling system' J.Chem.Eng.Jap. 17,52-57 (1984); Pan, Q.W., Wang, R.Z., Wang, L.W. and Liu, D. 'Design and experimental study of a silica gel-water adsorption chiller with modular adsorbers' Internat.J.Refrig. 67,336-344 (2016)

[5] Rezk, A. 'Effects of contact resistance and metal additives in finned-tube adsorbent beds on the performance of silica gel/water adsorption chiller' Appl.Thermal Eng. 53,278-284 (2013)

[6] Bauer, J. 'Zeolite/aluminum composite adsorbents for application in adsorption refrigeration' Internat.J.Energy Res. 33,1233-1249 (2009)

[7] Zhu, R. 'Experimental investigation on an adsorption system for producing chilled water' Rev.Int.Froid 15,(1),31-34 (1992)

[8] Wang, J.Y., Wang, R.Z. and Wang, L.W. 'Water vapor sorption performance of ACF-$CaCl_2$ and silica gel-$CaCl_2$ composite adsorbents' Appl.Therm.Energy 100,893-901 (2016); Tso, C.Y. 'Performance analysis of a waste heat driven activated carbon based composite adsorbent – Water adsorption chiller using simulation model' Internat.J. Heat Mass Tranf. 55,7596-7610 (2012)

[9] Lu, Z.S. 'Performance improvement and comparison of mass recovery in $CaCl_2$/activated carbon adsorption refrigerator and silica gel/LiCl adsorption chiller driven by low grade waste heat' Internat.J.Refrig. 36,1504-1511 (2013)

[10] Choudhury, B. 'An overview of developments in adsorption refrigeration systems towards a sustainable way of cooling' Appl.Energy 104,554-567 (2013)

[11] Galaev, I. Smart Polymers for Bioseparation and Bioprocessing CRC Press,(2001)

[12] Fundueanu, G. 'Poly(vinyl alcohol) microspheres with pH- and thermosensitive properties as temperature-controlled drug delivery' Acta Biomat. 6,3899-3907 (2010)

[13] Pelton, R. 'Poly(N-isopropylacrylamide) (PNIPAM) is never hydrophobic' J.Coll.Interf.Sci. 348,673-674 (2010)

[14] Morimoto, N. 'You have full text access to this content thermo-responsive hydrogels with nanodomains: rapid shrinking of a nanogel-crosslinking hydrogel of poly(N-isopropyl acrylamide)' Macromol. Rap. Comm. 29,672-676 (2008)

[15] Rotzetter, A.C.C. 'Thermoresponsive polymer induced sweating surfaces as an efficient way to passively cool buildings' Adv. Mater. 24,5352-5356 (2012)

[16] Teyssier, J., Saenko, S.V., van der Marel, D. and Milinkovitch, M.C. 'Photonic crystals cause active colour change in chameleons' Nat.Commun. 6, AR 6368 (2015)

[17] Bendiganavale, A.K. 'Infrared reflective inorganic pigments' Rec.Pat.Chem.Eng. 1,67-79 (2008)

[18] Peng, Z. 'A thermal degradation mechanism of polyvinyl alcohol/silica nanocomposites' Polym.Deg.Stab. 92,1061-1071 (2007)

[19] DeMerlis, C.C. 'Review of the oral toxicity of polyvinyl alcohol (PVA)' Food Chem.Tech. 41,319-326 (2003)

[20] Pielichowska, K. 'Phase change materials for thermal energy storage' Progr.Mater.Sci. 65,67-123 (2014)

[21] Muscatello, M.M.W. 'Poly(vinyl alcohol) rehydratable photonic crystal sensor materials' Adv.Funct.Mater. 18,1186-1193 (2008)

[22] Sinha, A. 'Biomimetic patterning of polymer hydrogels with hydroxyapatite nanoparticles' Mater. Sci. Eng. C 29,1330-1333 (2009)

[23] Peresin, M.S. 'Effect of moisture on electrospun nanofiber composites of poly(vinyl alcohol) and cellulose nanocrystals' Biomacromolecules 11,2471-2477 (2010); M.Penza 'Relative humidity sensing by PVA-coated dual resonator SAW oscillator' Sens.Act. 68B,300-306 (2000)

[24] Stober, W., Fink, A. and Bohn, E. 'Controlled growth of monodisperse silica spheres in the micron size range' J.Coll.Interf.Sci., 26, 62-69 (1968); Yao, L-F., Shi, Y., Jin, S-R., Li, M-J. and Zhang, L-M. 'The preparation of TiO_2/SiO_2 composite hollow spheres with hydrophobic inner surface and their application in controlled release' Mater.Res.Bull. 45,1351-1356 (2010)

[25] Gorsd, M. N., Blanco, M. N. and Pizzio L. R. 'Synthesis of polystyrene microspheres to be used as template in the preparation of hollow spherical materials: study of the operative variables' Procedia Mater.Sci. 1,432-438 (2012); Guojin, L., Zhou, L., Wu, Y., Wang, C., Fan, Q. and Shao, J. 'The fabrication of full color P(St-MAA) photonic crystal structure on polyester fabrics by vertical deposition self-assembly' J.Appl.Polym.Sci. 132,41750 (2015)

[26] Hua, Z., Yang, B., Chen, W., Bai, X., Xu, Q. and Gu, H. 'Surface functionalized magnetic PVA microspheres for rapid naked-eye recognizing of copper(II) ions in aqueous solutions' Appl.Surf.Sci. 317,226-235 (2014)

[27] Ahmad, H., Nurunnabi, M., Rahman M. M., Kumar, K., Tauer, K., Minami, H., Gafur, M. A., 'Magnetically doped multi stimuli-responsive hydrogel microspheres with IPN structure and application in dye removal' Coll.Surf. 459A,39–47 (2014)

[28] Valentín, J.L., López, D., Hernández, R., Mijangos, C., Saalwächter, K. 'Structure of Poly(vinyl alcohol) Cryo-Hydrogels as Studied by Proton Low-Field NMR Spectroscopy' Macromolecules 42,263-272 (2009)

[29] Zhang, Q. 'Effect of poly(vinyl alcohol) coating process conditions on the properties and performance of polyamide reverse osmosis membranes' Desalination 379,42-52 (2016)

[30] Wang, Q., 'Tunable optical nanoantennas incorporating bowtie nanoantenna arrays with stimuli-responsive polymer' Sci.Rep. 5,18567 (2015)

[31] Ferral, H., 'Hydrogel-Coated Coils: Product Description and Clinical Applications.' Sem.Inter.Radio. 32,343-348 (2015)

[32] Du, X., 'Metal ion-responsive photonic colloidal crystalline micro-beads with electrochemically tunable photonic diffraction colours' Sens.Acuat. 223B,318-323 (2016)